

Non-parametric frequency response estimation using a local rational model ¹

Tomas McKelvey* and Guillaume Guérin**

* Dept. of Signals and Systems, Chalmers University of Technology,
 SE-412 96 Gothenburg, Sweden, mckelvey@chalmers.se

** ENSEIRB-MATMECA, Université de Bordeaux, France,
 guillaume.guerin@enseirb-matmeca.fr

Abstract: A review of the relationship between the frequency response function of linear system and the DFT of the input and output signals show that the output DFT is a sum of two terms. The first term contain the FRF multiplied with the input DFT and the second term capture the effect when the system is not operating in a periodic fashion. The utilization of these two terms when performing non-parametric frequency response estimation has led to the previously developed Local Polynomial Method. This paper acknowledge that the two terms can better be approximated by local rational functions with a common denominator polynomial and a new method called Local Rational Method has been developed. Numerical simulations illustrate the performance of the new rational method in comparison with the polynomial one. The results suggest that the new rational method gives better performance when the system has a resonant behavior.

Keywords: system identification, discrete Fourier transform, frequency response, estimation, local models, estimation algorithms

1. INTRODUCTION

The frequency response function (FRF) is a key component in many domains for system analysis and design. Given experimental measurements from a system it is thus highly desirable to derive a high quality estimate of the FRF without imposing assumptions which will reduce the flexibility to accurately reproduce the true FRF. In principle there are two issues which need to be balanced when estimating a FRF. The complexity of the FRF itself and the noise in the data record. In parametric modeling a low order model is fitted to the data where the number of estimated parameters are significantly fewer than the length of the data record. If the true system is a member of the low order model structure a very high quality estimate of the FRF is possible. In non-parametric modeling the number of estimated parameters are of the same order as the length of the data record enabling a very flexible model but with a much higher sensitivity to noise.

The empirical transfer function estimate (ETF) is a very simple non-parametric FRF estimate employing the Discrete Fourier Transform (DFT). The FRF estimate at DFT frequency k is formed by dividing the DFT of the output with the DFT of the input. The leakage effects inherent in Discrete Fourier Transform (DFT) of non-periodic signals will yield a systematic error unless the input is periodic and the measurement record has a length equal to the period length. To mitigate these effects techniques from spectral analysis have been employed to smooth the estimate of the signal level, see e.g. Brillinger [1981], Ljung [1999], Wellstead [1981]

By also taking into account the linear system relation it is possible to mitigate the leakage effects by explicit modeling. This has been utilized for parametric system identification in the frequency domain Pintelon et al. [1997], Schoukens et al. [1999], McKelvey [2000, 2002]. Recently the Local Polynomial Method (LPM) has been

presented which employ polynomials to explicitly model the leakage effects for non-parametric FRF estimation, see Schoukens et al. [2009]. In this paper this method is extended to utilize local rational models to better capture FRF from resonant systems.

In the next section the relationship between the DFT of the input and output signals are carefully reviewed and form a basis for the development of a new method in Section 3. Numerical simulations are presented and discussed in Section 4 and conclusions are given in the final section.

2. FREQUENCY RESPONSE FUNCTION

This section is devoted to an analysis of data from linear systems using the Discrete Fourier Transform (DFT). In this section noise effects are not discussed and we return to this issue when describing the estimation problem.

The output of a general discrete time causal linear system is given by the relation

$$y(t) = \sum_{k=0}^{\infty} g(k)u(t-k) \quad (1)$$

where $u(t)$ is the input signal and $g(k)$ is the impulse response of the system. The discrete time Fourier transform (DTFT) of a signal $x(t)$ is defined by

$$X(\omega) \triangleq \sum_{t=-\infty}^{\infty} x(t)e^{-j\omega t} \quad (2)$$

Here $X(\omega)$ is a 2π -periodic complex function. The inverse transform is given by

$$x(t) = \frac{1}{2\pi} \int_0^{2\pi} X(\omega)e^{j\omega t} d\omega \quad (3)$$

It is well known that the convolution equation (1) can be expressed as a multiplication in the Fourier domain

$$Y(\omega) = G(\omega)U(\omega). \quad (4)$$

¹ This work was sponsored by the Swedish Research Council (VR) which is gratefully acknowledged.

where the DTFT of the impulse response, $G(\omega)$, is called the frequency response function (FRF) of the linear system. Given $Y(\omega)$ and $U(\omega)$ it is from (4) straight-forward to derive the FRF. However, in reality only a finite amount of input-output data is available which makes it impossible to directly employ (4) to calculate the FRF.

The discrete Fourier transform (DFT) is the practical tool to perform Fourier analysis based on finite length data records. The N -point DFT is defined as

$$X(k) \triangleq \sum_{t=0}^{N-1} x(t)e^{-j2\pi kt/N} \quad (5)$$

for $k = 0, 1, \dots, N-1$ which imply the inverse is given by

$$x(t) = \frac{1}{N} \sum_{k=0}^{N-1} X(k)e^{j2\pi kt/N} \quad (6)$$

$t = 0, 1, \dots, N-1$. The DFT is a linear invertible transformation in the space \mathbb{C}^N . We use the notational convention that an integer argument, k , to $X(\cdot)$ refers to the DFT while a real argument ω refers to the DTFT. The connection between the DFT and the DTFT can directly be established for a few cases. First, if the signal $x(t)$ is identically zero outside the interval $0 \leq t < N$. Then it is clear by comparing (2) and (5) that

$$X(k) = X(\omega_k), \quad \text{where } \omega_k = 2\pi k/N. \quad (7)$$

Hence, in this case the DFT are discrete values of the continuous DTFT.

If $x(t)$ is a periodic signal with period N , the signal energy is infinite and the classical DTFT does not exist. However, using distributions the theory can be extended to also include sinusoidal signals. Hence if $x(t) = e^{j\omega_0 t}$ then $X(\omega) = 2\pi\delta(\omega - \omega_0)$ where $\delta(\cdot)$ is the Dirac delta function. The IDFT in (6) is indeed a complex Fourier series representation of a periodic signal and the DTFT for a periodic signal is given by

$$X(\omega) = \frac{1}{N} \sum_{k=0}^{N-1} X(k)2\pi\delta(\omega - 2\pi k/N) \quad (8)$$

Three distinct cases can be identified where different assumptions are made based on the character of the input and the linear system.

Case 1: Periodic input. Employing the DTFT representation (8) of a periodic input with period N and the relation (4) we obtain the output DTFT as

$$Y(\omega) = \frac{1}{N} \sum_{k=0}^{N-1} G(\omega)U(k)2\pi\delta(\omega - 2\pi k/N) \quad (9)$$

after an inverse DTFT we obtain

$$y(t) = \frac{1}{N} \sum_{k=0}^{N-1} G(\omega_k)U(k)e^{j2\pi kt/N} \quad (10)$$

where $\omega_k = 2\pi k/N$. Clearly, (10) is a complex Fourier series representation of a periodic signal. Hence, $y(t)$ is periodic with period N . Furthermore the DFT of one period of $y(t)$ is

$$Y(k) = G(\omega_k)U(k). \quad (11)$$

Case 2: Finite length input If the input has a finite duration of N samples the DTFT-DFT relation is given by (7). The resulting output though is in general not zero

at $t = N$ and beyond. However, for stable systems the response beyond $t = N-1$ will decay at the same rate as the impulse response. For systems with a finite impulse response of length N_h the output has a finite non-zero duration for at most $N + N_h - 1$ time instances. If we zero-pad the input and impulse response sequences to a total length of $N + N_h - 1$ and then calculate the $N + N_h - 1$ points DFT we obtain

$$Y(k) = G(k)U(k) \quad (12)$$

for $k = 0, 1, \dots, N + N_h - 2$. If the system has an infinite impulse response an approximation is obtained if N_h is selected such that the impulse response has decayed significantly.

Case 3: Arbitrary input The third case considers a common situation where a plant, or system is operating with an arbitrary input and it is not possible to set the input to zero for large portions of time nor make the input periodic. This means that the output will always be subject not only to the present input sequence but also past sequences, which are not known to us. A finite linear model of arbitrary order will be used to analyze this case. Assume the causal discrete time linear system has a finite McMillan degree n . Then it can be described by a state space model of order n , see Kailath [1980]:

$$\begin{aligned} \mathbf{x}(t+1) &= \mathbf{A}\mathbf{x}(t) + \mathbf{B}u(t) \\ y(t) &= \mathbf{C}\mathbf{x}(t) + \mathbf{D}u(t) \end{aligned} \quad (13)$$

where $\mathbf{x}(t) \in \mathbb{R}^n$ is the state vector. Now the N -point DFT of $\mathbf{x}(t+1)$ is

$$\sum_{t=0}^{N-1} \mathbf{x}(t+1)e^{-\frac{j2\pi kt}{N}} = e^{\frac{j2\pi k}{N}} (\mathbf{X}(k) + \mathbf{x}(N) - \mathbf{x}(0)) \quad (14)$$

Employing the N -point DFT on the two equations in the state space model yields

$$\begin{aligned} e^{\frac{j2\pi k}{N}} (\mathbf{X}(k) + \mathbf{x}(N) - \mathbf{x}(0)) &= \mathbf{A}\mathbf{X}(k) + \mathbf{B}U(k) \\ Y(k) &= \mathbf{C}\mathbf{X}(k) + \mathbf{D}U(k) \end{aligned} \quad (15)$$

By eliminating the state from the state-space equations the DFT input-output relation for an arbitrary input is obtained as

$$Y(k) = G(\omega_k)U(k) + T(\omega_k) \quad (16)$$

where

$$\begin{aligned} G(\omega_k) &= \mathbf{D} + \mathbf{C}(e^{j\omega_k \mathbf{I}} - \mathbf{A})^{-1}\mathbf{B} \\ T(\omega_k) &= \mathbf{C}(e^{j\omega_k \mathbf{I}} - \mathbf{A})^{-1}(\mathbf{x}(0) - \mathbf{x}(N))e^{j\omega_k} \end{aligned} \quad (17)$$

and $\omega_k = 2\pi k/N$. This result shows that the DFT-relation between the input and output can be expressed as the summation of the effect of the input, $G(\omega_k)U(k)$, and a second term $T(\omega_k)$. This result was presented in a polynomial context by Pintelon et al. [1996, 1997], Schoukens et al. [1999] and in a state-space context by McKelvey [2000]. Investigating (17), it can be noted that $G(\omega_k)$ is the frequency function of the state-space model in (13). Furthermore the extra term $T(\omega_k)$ has the same dynamics, i.e. poles, as the state-space model. One interpretation is that $T(\omega_k)$ represents the effect of an additional additive unit input which is non-zero only for $t = -1$, since the DTFT of such a signal is $e^{j\omega}$. This extra input effect the state-equation through the " \mathbf{B} " vector defined by $\mathbf{x}(0) - \mathbf{x}(N)$. The effect of this artificial input is to move the state at $t = 0$ to a value equal to the value which would have been obtained if the input $u(t)$ would have been a true N -periodic signal.

The description in (16) of course also applies to the two previously described cases. For Case 1 with a periodic

input we directly note that $\mathbf{x}(0) - \mathbf{x}(N) = 0$ and hence $T(\omega_k) \equiv 0$. For Case 2 we first assumed the input is finite and hence $u(t) = 0$ for $n < 0$ hence $\mathbf{x}(0) = 0$. Secondly it was also assumed the output was zero for $t \geq N$ which then implies $\mathbf{x}(N) = 0$ and consequently $T(\omega_k) \equiv 0$ also for this case.

Finally, it is also worth pointing out that the theoretical discussion above has not made any assumption on the size of the input and output signals and the results are thus also valid for multivariable systems without any change of notation.

3. LOCAL FRF MODELING

Estimating the frequency response function of a linear system based on a data record of samples of the input and output can be made with in different ways. In the parametric approach a model class of low order is assigned and the parameters of the model are determined by a numerical algorithm based on arguments based on approximation, statistical or geometrical properties. In a non-parametric approach the frequency function is estimated locally by employing various smoothing techniques to reduce noise and bias effects. An overview of both approaches can be found in many books e.g. Ljung [1999], Söderström and Stoica [1989], Pintelon and Schoukens [2001].

In this section we assume the following data and system model

$$y(t) = \sum_{k=0}^{\infty} g(k)u(t-k) + v(t) \quad (18)$$

where as before $g(k)$ is the impulse response and $v(t)$ is a zero-mean stochastic process modeling the measurement and process noise. The input $u(t)$ and measured output $y(t)$ are assumed known in the interval $t = 0, 1, \dots, N-1$. Furthermore $Y(k)$ and $U(k)$ denote the N -point DFT of the signals respectively and $V(k)$ denote the N -point DFT of the disturbance $v(t)$. Finally $\omega_k \triangleq 2\pi k/N$.

The classical approach to local FRF modeling is known as the Empirical Transfer Function Estimate (ETFTE). In its simplest form the estimate is given by

$$\hat{G}_{\text{ETFTE}}(\omega_k) = \frac{Y(k)}{U(k)}. \quad (19)$$

This estimate has good properties only when the input is periodic (Case 1) or when input and output are zero outside the interval (Case 2) and $|U(k)|$ is not too small. In this case we have

$$\hat{G}_{\text{ETFTE}}(\omega_k) = \frac{Y(k)}{U(k)} = G(\omega_k) + \frac{V(k)}{U(k)}. \quad (20)$$

Clearly if $|U(k)|$ is close to zero for some k the FRF estimate at that frequency will be dominated by the noise term. In order to improve this problem the estimate can be smoothed by also employing values at neighboring frequencies in the estimate, see e.g. Chapter 6.4 in Ljung [1999]. These techniques has also been used for data records not collected in circumstances when Case 1 or Case 2 are applicable. For such cases an additional term will end up in the FRF estimate as illustrated in the previous section.

$$\hat{G}_{\text{ETFTE}}(\omega_k) = \frac{Y(k)}{U(k)} = G(\omega_k) + \frac{T(\omega_k)}{U(k)} + \frac{V(k)}{U(k)} \quad (21)$$

which will add additional errors in the FRF estimate.

However, it is only recently that the structure of the addition term, the transient term, $T(\omega_k)$ has been utilized for non-parametric estimation. Clearly, it is impossible

to uniquely estimate both $G(\omega_k)$ and $T(\omega_k)$ based only on the values $Y(k)$ and $U(k)$ for a single frequency k . Instead we must add an assumption that the function values for nearby frequencies are closely related for the system frequency response functions and the transient term. The analysis of Case 3 above show that not only the FRF $G(\omega)$ but also the transient frequency function $T(\omega)$ is a rational function of the same dimension as the true system. Frequency response functions for most systems are smooth and hence local smoothing can be applied not only for $G(\omega_k)$ but also $T(\omega_k)$. In Schoukens et al. [2009] a new method known as the Local Polynomial Method (LPM) was developed. In LPM local polynomial models are estimated both for the FRF and the transient term simultaneously. This technique improve the FRF estimation quality significantly as compared to the standard ETFTE. In LPM the frequency response and transient term are modeled locally around the DFT frequency k as

$$\begin{aligned} G_{k+r} &= \sum_{s=0}^R g_s(k)r^s \\ T_{k+r} &= \sum_{s=0}^R t_s(k)r^s \end{aligned} \quad (22)$$

Let θ_k be a vector comprising the parameters $\{g_s(k)\}_{s=0}^R$ and $\{t_s(k)\}_{s=0}^R$. The parameters of the local model for DFT frequency k are estimated by minimizing the least-squares problem

$$\hat{\theta}_k \triangleq \arg \min_{\theta_k} \sum_{r=-N_w}^{N_w} |Y(k+r) - G_{k+r}U(k+r) - T_{k+r}|^2 \quad (23)$$

over a frequency window symmetric around k and of total length $2N_w + 1$. The LMP frequency response estimate is then simply

$$\hat{G}_{\text{LPM}}(k) \triangleq \hat{G}_{k+0} = \hat{g}_0(k). \quad (24)$$

This optimization is repeated for all frequencies in the DFT grid.

Returning back to the assumption underlying the success of the LPM method reveals that the smoothness of the functions are essential. The polynomial model is suitable when the local behavior of the functions can be well approximated by polynomials. If this is not a good approximation other local model structures could lead to better results. If we consider finite dimensional models with poles close to the unit circle the frequency response function have peaks which are not well modeled by a polynomial function. Instead we propose to use local rational models both for G and T . Since the analysis revealed that G and T have the same poles it is natural to incorporate this also in the local model. We propose the following local rational method (LRM) where the local model (22) is extended as follows.

$$\begin{aligned} G_{k+r} &= \frac{N_{k+r}}{D_{k+r}} \\ T_{k+r} &= \frac{M_{k+r}}{D_{k+r}} \end{aligned} \quad (25)$$

where

$$\begin{aligned}
 N_{k+r} &= \sum_{s=0}^R n_s(k)r^s \\
 D_{k+r} &= 1 + \sum_{s=1}^R d_s(k)r^s \\
 M_{k+r} &= \sum_{s=0}^R m_s(k)r^s
 \end{aligned} \quad (26)$$

The vector θ_k is defined to be a vector with the local rational model parameters $\{n_s(k)\}_{s=0}^R$ and $\{d_s(k)\}_{s=0}^R$ and $\{m_s(k)\}_{s=1}^R$. The local model linking $Y(k)$ with $U(k)$ can now be expressed as

$$Y(k+r) = \frac{N_{k+r}}{D_{k+r}}U(k+r) + \frac{M_{k+r}}{D_{k+r}} + V(k+r). \quad (27)$$

The parameters of the rational local model are not linear in G_{k+r} and T_{k+r} . However, by multiplying the equation with D_{k+r} all parameters appear linear in the equation and the parameters can be estimated by solving the equation in a least-squares sense.

$$\begin{aligned}
 \hat{\theta}_k = \arg \min_{\theta_k} & \sum_{r=-N_w}^{N_w} |Y(k+r)D_{k+r} \\
 & - N_{k+r}U(k+r) - M_{k+r}|^2 \quad (28)
 \end{aligned}$$

The Local Rational Method estimate of the FRF at frequency k is then defined by

$$\hat{G}_{\text{LRM}}(k) \triangleq \hat{G}_{k+0} = \frac{\hat{N}_{k+0}}{\hat{D}_{k+0}} = \hat{n}_0(k) \quad (29)$$

The total number of parameters to be estimated is $3R+2$. A necessary condition for the LS-problem to have a unique solution is that the window size N_w is selected such that

$$2N_w + 1 \geq 3R + 2. \quad (30)$$

For LPM the requirement on the window size is

$$2N_w + 1 \geq 2R + 2. \quad (31)$$

The N -periodic property of $Y(k)$ and $U(k)$ is utilized when the index summations $(k+r)$ in (28) are negative, i.e. $Y(-1) = Y(N-1)$, $Y(-2) = Y(N-2)$, etc.

4. SIMULATION RESULTS

In this section results from numerical Monte-Carlo simulations are presented to highlight some properties of the proposed LRM. Two related example systems will be used for data generation. Both systems are of order 8 and are constructed by adding 4 second order resonant sub-systems. The pole locations of the four sub-systems are given by

$$\begin{aligned}
 p_1 &= \rho e^{\pm j2\pi 0.1}, & p_2 &= \rho e^{\pm j2\pi 0.11} \\
 p_3 &= \rho e^{\pm j2\pi 0.2}, & p_4 &= \rho e^{\pm j2\pi 0.3}
 \end{aligned} \quad (32)$$

None of the four subsystems have any zeros and the gain is adjusted to obtain a unit DC-gain for each subsystem. The time domain noise signal is a zero-mean, temporally white normally distributed random variable with standard deviation σ_v . The input to the system is selected as a zero-mean, temporally white normally distributed random variable with a unit standard deviation. The system is driven by an input signal of length 2048. The first 1024 samples of the input and output signals are discarded and the remaining $N = 1024$ are used for the estimation. In each Monte-Carlo run a new input and a new noise realization are generated. Five different experiments E1 to E5, have been performed where the magnitude of the pole location, ρ have been varied between 0.9 and 0.98

Table 1. RMS magnitude error values for the five different simulations cases. The squared magnitude error is averaged over both the Monte-Carlo simulations and over frequencies.

RMSE	ETFE	LPM	LRM
E1 $\rho = 0.9, \sigma_v = 0$	0.16	3.2E-3	7.9E-6
E2 $\rho = 0.9, \sigma_v = 0.01$	0.12	8.2E-3	12E-3
E3 $\rho = 0.98, \sigma_v = 0$	0.42	0.73	326E-6
E4 $\rho = 0.98, \sigma_v = 0.01$	0.64	0.72	0.012
E5 as E4 but $N_w = 8$ for LRM	0.33	0.73	5.5E-3

and the noise level has been changed between noise-free case $\sigma_v = 0$ and $\sigma_v = 0.01$. During all experiments the local model order has been kept constant at a value of $R = 2$. During the first four experiments the window size has been selected to $N_w = 4$ for both methods while in the fifth experiment N_w was increased to 8 for LRM. To obtain a scalar measure of the performance the root mean square of the error magnitude has been calculated where the average is over all frequencies and all Monte-Carlo runs. The RMSE results are presented in Table 1. In Figures 1 to 5 the frequency response function $G(\omega)$ is shown as the blue graph, the RMS estimation error magnitude for ETFE, LPM and LRM are shown as green, red and cyan graphs respectively.

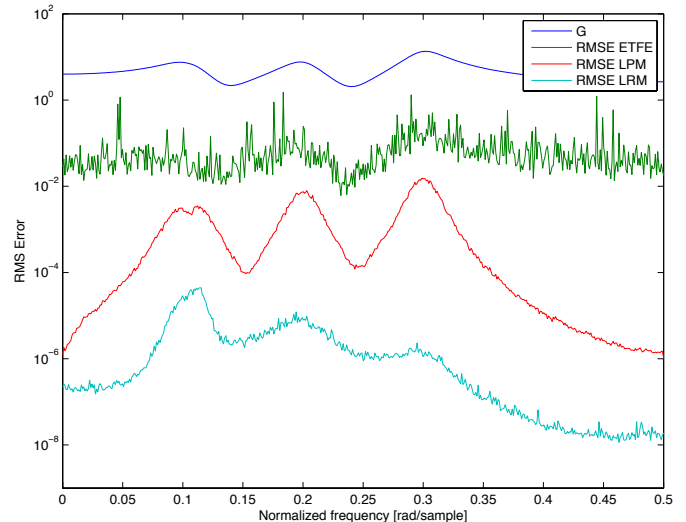


Fig. 1. Experiment 1, $\rho = 0.9, \sigma_v = 0$: Blue graph is the true frequency response function. RMS magnitude error for the estimation methods, ETFE, LPM and LRM are shown as green, red and cyan graphs respectively.

4.1 Discussion

LRM is a more flexible model structure since it has more parameters to be estimated. This is clearly evident in both Experiment 1 and 3 since the RMSE error is uniformly lower for LRM compared to LPM when the data is noise free, i.e. the bias error is less for LRM than LPM. When noise is added as in Experiment 2 we notice that LPM has lower RMSE for most frequencies. The estimation variance increases with a more flexible model and here the total error for LRM is larger. Since the window size N_w is equal for both methods it is expected that the noise will influence the LRM more than LPM. However, when the system has a FRF with sharper peaks the bias error at the peak locations for LPM are even larger than the ETFE as clearly seen in Figure 3. Even with noise added this bias error dominates around the peaks. Far away from the peaks LPM has the lowest RMSE again due to fewer estimated parameters. Since the LRM has a low

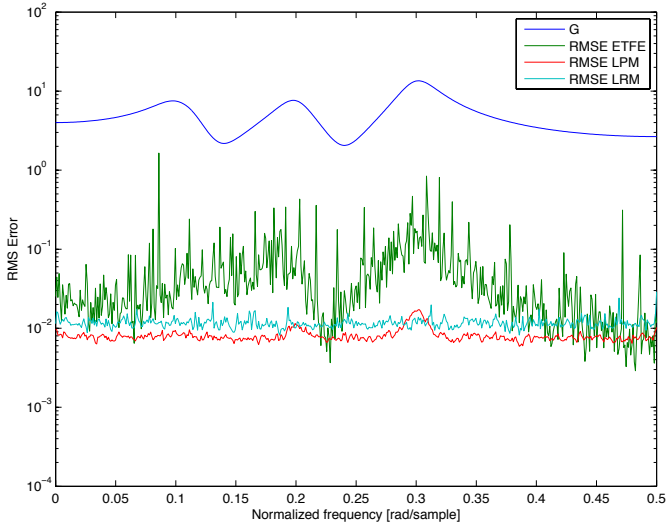


Fig. 2. Experiment 2, $\rho = 0.9$, $\sigma_v = 0.01$: Blue graph is the true frequency response function. RMS magnitude error for the estimation methods, ETFE, LPM and LRM are shown as green, red and cyan graphs respectively.

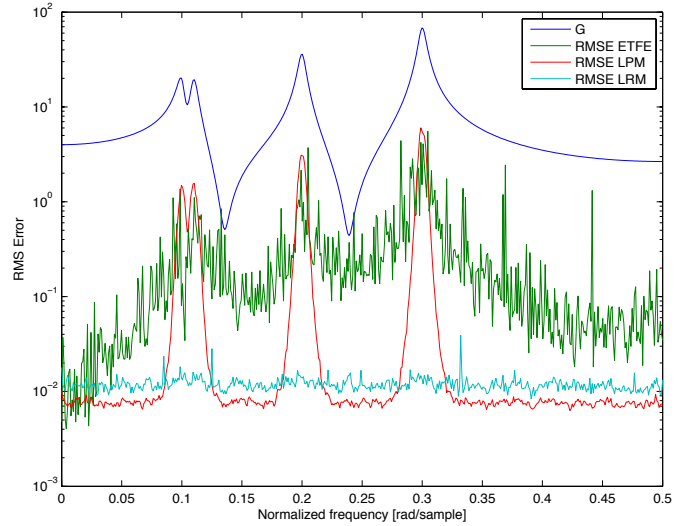


Fig. 4. Experiment 4, $\rho = 0.98$, $\sigma_v = 0.01$: Blue graph is the true frequency response function. RMS magnitude error for the estimation methods, ETFE, LPM and LRM are shown as green, red and cyan graphs respectively.

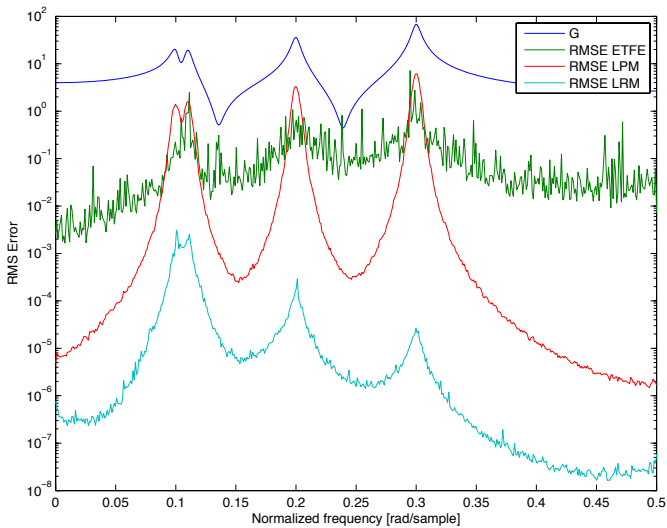


Fig. 3. Experiment 3, $\rho = 0.98$, $\sigma_v = 0$: Blue graph is the true frequency response function. RMS magnitude error for the estimation methods, ETFE, LPM and LRM are shown as green, red and cyan graphs respectively.

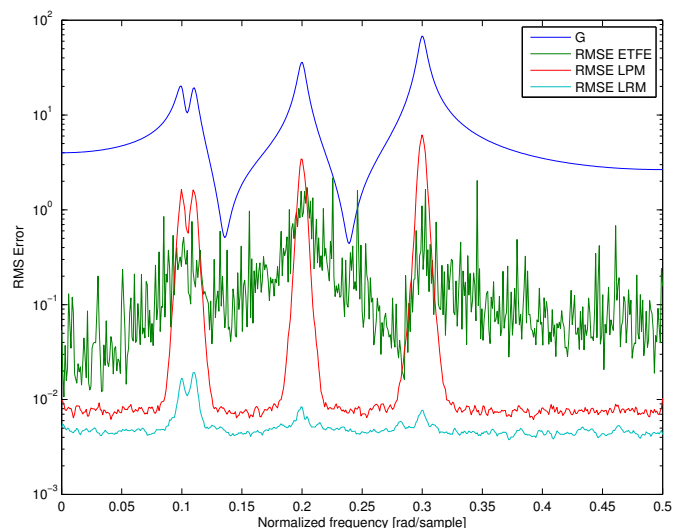


Fig. 5. Experiment 5, $\rho = 0.98$, $\sigma_v = 0.01$, $N_w = 8$ for LRM and $N_w = 4$ for LPM: Blue graph is the true frequency response function. RMS magnitude error for the estimation methods, ETFE, LPM and LRM are shown as green, red and cyan graphs respectively.

bias error it is possible to improve the situation further by allowing for a larger estimation window in order to try to balance the variance and bias error. Experiment 5 illustrates the effect where now LRM has a uniformly lower RMS magnitude error than the LPM. The results suggest that usage of the rational method is highly beneficial when the system has resonant behavior.

5. CONCLUSIONS

A review of the relationship between the FRF of a system and the DFT of an input and output sequence illustrate that the output DFT is a sum of two terms. The first term contain the FRF multiplied with the input DFT and the second term capture the effect when the system is not operating in a periodic fashion. The utilization of these two terms when performing non-parametric estimation has led to the previously developed Local Polynomial Method.

This paper acknowledge that the two terms indeed can be approximated by rational functions with a common denominator polynomial and a new method called Local Rational Method has been developed. Numerical simulations illustrate the performance of the new rational method in comparison with the polynomial one and the results suggest that the new rational method gives better performance when the system has a resonant behavior.

REFERENCES

- D. R. Brillinger. *Time Series: Data Analysis and Theory*. McGraw-Hill Inc., New York, 1981.
- T. Kailath. *Linear Systems*. Prentice-Hall, Englewood Cliffs, New Jersey, 1980.
- L. Ljung. *System Identification: Theory for the User*. Prentice-Hall, Englewood Cliffs, New Jersey, second edition, 1999.

- T. McKelvey. Frequency domain identification. In R. Smith and D. Seborg, editors, *Preprints of the 12th IFAC Symposium on System Identification*, Santa Barbara, CA, USA, June 2000. Plenary paper.
- T. McKelvey. Frequency domain identification methods. *Circuits Systems Signal Processing*, 21(1):39–55, 2002.
- R. Pintelon and J. Schoukens. *System Identification - A frequency domain approach*. IEEE Press, 2001.
- R. Pintelon, J. Schoukens, and G. Vandersteen. Frequency domain system identification using arbitrary signals. In *Proc. 35th IEEE Conference on Decision and Control, Kobe, Japan*, volume 2, pages 2048–2051, Dec 1996.
- R. Pintelon, J. Schoukens, and G. Vandersteen. Frequency domain system identification using arbitrary signals. *IEEE Trans. on Automatic Control*, 42(12):1717–1720, Dec 1997.
- J. Schoukens, G. Vandersteen, R. Pintelon, and P. Guillaume. Frequency-domain identification of linear systems using arbitrary excitations and a nonparametric noise model. *IEEE Trans. on Automatic Control*, AC-44(2):343–347, 1999.
- J. Schoukens, G. Vandersteen, K. Barbe, and R. Pintelon. Nonparametric preprocessing in system identification: a powerful tool. *European Journal of Control*, 15:260–274, 2009.
- T. Söderström and P. Stoica. *System Identification*. Prentice-Hall International, Hemel Hempstead, Hertfordshire, 1989.
- P.E. Wellstead. Non-parametric methods of system identification. *Automatica*, 14:89–91, 1981.